Rotating regularized Schwarzschild and JNW spacetimes as Kerr Black hole mimickers

Rajibul Shaikh

SeoulTech, Seoul, S. Korea

High1 Workshop on Particle, String and Cosmology
High1, S. Korea

January 21-27, 2024

Background image courtesy: https://eventhorizontelescope.org/

Based on

- **R. Shaikh**, P. Kocherlakota, R. Narayan, and P. S. Joshi, *Shadows of spherically symmetric black holes and naked singularities*, MNRAS **482**, 52-64 (2019).
- **R. Shaikh**, K. Pal, K. Pal, and T. Sarkar, *Constraining alternatives to the Kerr black hole*, MNRAS **506**, 1229-1236 (2021).
- **R. Shaikh**, *Testing black hole mimickers with the Event Horizon Telescope image of Sagittarius A**, MNRAS **523**, 375-384 (2023).
- K. Pal, K. Pal, **R. Shaikh**, and T. Sarkar, *A rotating modified JNW spacetime as a Kerr black hole mimicker*, JCAP 11 (2023) 060.

Motivations

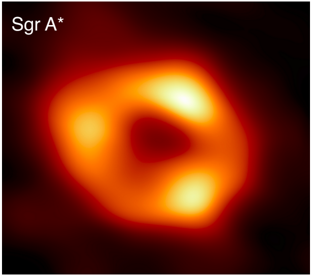

Motivations

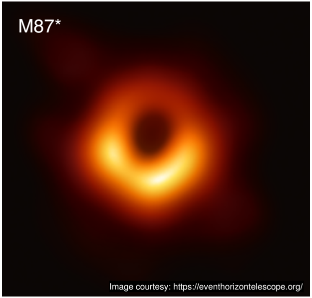

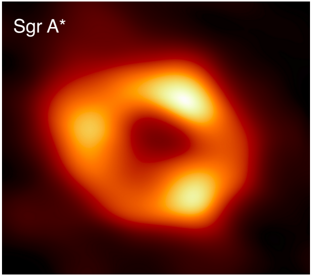

- It is commonly believed that the gravitational field around astrophysical compact objects is described by the Kerr black hole geometry.
- According to the Event Horizon Telescope (EHT) collaboration, the expected appearance of the Kerr black hole is consistent with the observed images and shadows.

Motivations

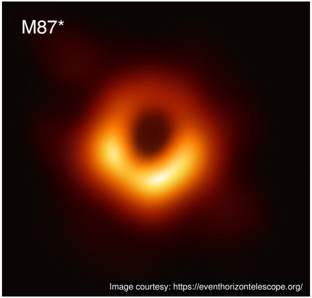

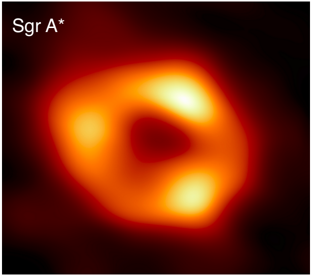

- It is commonly believed that the gravitational field around astrophysical compact objects is described by the Kerr black hole geometry.
- According to the Event Horizon Telescope (EHT) collaboration, the expected appearance of the Kerr black hole is consistent with the observed images and shadows.
- However, as we shall see, compact objects which do not have singularities or event horizons can also cast black-hole-like shadows, thereby acting as black hole mimickers.
- Based on shadow observations, these mimickers can not be ruled out completely at the current stage.

Motivations

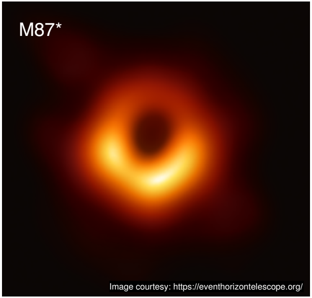

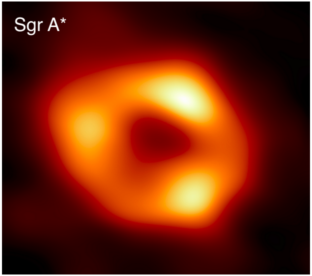

- It is commonly believed that the gravitational field around astrophysical compact objects is described by the Kerr black hole geometry.
- According to the Event Horizon Telescope (EHT) collaboration, the expected appearance of the Kerr black hole is consistent with the observed images and shadows.
- However, as we shall see, compact objects which do not have singularities or event horizons can also cast black-hole-like shadows, thereby acting as black hole mimickers.
- Based on shadow observations, these mimickers can not be ruled out completely at the current stage.
- We consider rotating versions of regularized Schwarzschild and JNW spacetimes and constrain them using the EHT results.

Motivations

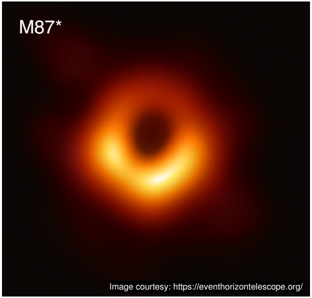

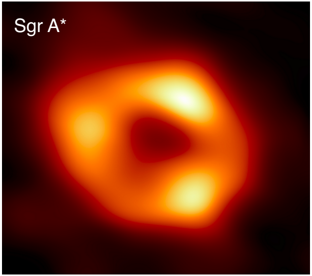

- It is commonly believed that the gravitational field around astrophysical compact objects is described by the Kerr black hole geometry.
- According to the Event Horizon Telescope (EHT) collaboration, the expected appearance of the Kerr black hole is consistent with the observed images and shadows.
- However, as we shall see, compact objects which do not have singularities or event horizons can also cast black-hole-like shadows, thereby acting as black hole mimickers.
- Based on shadow observations, these mimickers can not be ruled out completely at the current stage.
- We consider rotating versions of regularized Schwarzschild and JNW spacetimes and constrain them using the EHT results.
- Recently, R. P. Kerr has argued that there is no proof that black holes contain singularities (arXiv:2312.00841).
  $\Rightarrow$ Added motivation to our work.

Rotating regularized Schwarzschild and JNW spacetimes

- Schwarzschild black hole metric

$$ds^2 = -\left(1 - \frac{2M}{r}\right) dt^2 + \frac{dr^2}{1 - \frac{2M}{r}} + r^2 \left(d\theta^2 + \sin^2\theta d\phi^2\right)$$

- Replace the singularity by a non-singular minimal surface of radius r_0 [A. Simpson and M. Visser, JCAP 1902 (2019) 042]

$$r \longrightarrow \sqrt{r^2 + r_0^2}$$

- Simpson-Visser metric

$$ds^2 = -\left(1 - \frac{2M}{\sqrt{r^2 + r_0^2}}\right) dt^2 + \frac{dr^2}{1 - \frac{2M}{\sqrt{r^2+r_0^2}}} + (r^2 + r_0^2)\left(d\theta^2 + \sin^2\theta d\phi^2\right)$$

- $r_0 \leq 2M \Rightarrow$ non-singular black hole, $r_0 > 2M \Rightarrow$ Wormhole (with throat radius r_0)

- Appears as an exact solution in a class of Scalar-Tensor Horndeski gravity theory (N. Chatzifotis, E. Papantonopoulos, and C. Vlachos, Phys. Rev. D 105, 064025 (2022)).

Rotating regularized Schwarzschild and JNW spacetimes

- We construct rotating version of the regularized Schwarzschild metric using Newman-Janis algorithm (**R. Shaikh**, K. Pal, K. Pal, and T. Sarkar, MNRAS **506**, 1229-1236 (2021))

$$
\begin{aligned}
ds^2 &= -\left(1-\frac{2Mr}{\Sigma}\right)dt^2 - \frac{4Mar\sin^2\theta}{\Sigma}dtd\phi + \frac{\Sigma}{\Delta\hat{\Delta}}dr^2 + \Sigma d\theta^2 \\
&+ \left(r^2+a^2+\frac{2Ma^2r\sin^2\theta}{\Sigma}\right)\sin^2\theta d\phi^2, \quad \hat{\Delta} = 1-\frac{r_0^2}{r^2}
\end{aligned}
$$

- The event horizon radii are given by $\Delta = 0$, i.e., $r_\pm = M \pm \sqrt{M^2-a^2}$.
- $r_0 \le r_+ \Rightarrow$ non-singular black hole, $r_0 > r_+ \Rightarrow$ Wormhole.

Rotating regularized Schwarzschild and JNW spacetimes

- We construct rotating version of the regularized Schwarzschild metric using Newman-Janis algorithm (**R. Shaikh**, K. Pal, K. Pal, and T. Sarkar, MNRAS **506**, 1229-1236 (2021))

$$
\begin{aligned}
ds^2 &= -\left(1-\frac{2Mr}{\Sigma}\right)dt^2 - \frac{4Mar\sin^2\theta}{\Sigma}dtd\phi + \frac{\Sigma}{\Delta\hat{\Delta}}dr^2 + \Sigma d\theta^2 \\
&+ \left(r^2+a^2+\frac{2Ma^2r\sin^2\theta}{\Sigma}\right)\sin^2\theta d\phi^2, \quad \hat{\Delta} = 1-\frac{r_0^2}{r^2}
\end{aligned}
$$

- The event horizon radii are given by $\Delta = 0$, i.e., $r_\pm = M \pm \sqrt{M^2-a^2}$.
- $r_0 \leq r_+ \Rightarrow$ non-singular black hole, $r_0 > r_+ \Rightarrow$ Wormhole.
- Janis-Newman-Winicour (JNW) metric

$$
ds^2 = -\left(1-\frac{2M}{\gamma r}\right)^{\gamma} dt^2 + \frac{dr^2}{\left(1-\frac{2M}{\gamma r}\right)^{\gamma}} + r^2\left(1-\frac{2M}{\gamma r}\right)^{1-\gamma}\left(d\theta^2+\sin^2\theta d\phi^2\right)
$$

- Solution in general relativity with minimally coupled scalar field.
- Naked singularity at $r = r_s = 2M/\gamma, \quad \gamma = 1 \Rightarrow$ Schwarzschild Black hole.
- We follow the same procedure to obtain the rotating regularized JNW metric (K. Pal, K. Pal, **R. Shaikh**, and T. Sarkar, JCAP 11 (2023) 060).
- $r_0 \leq r_s \Rightarrow$ Naked singularity, $\quad r_0 > r_s \Rightarrow$ Wormhole

Do only black holes cast shadows?

Shadow cast by a compact object

- Schwarzschild black hole metric

$$ds^2 = -\left(1 - \frac{2M}{r}\right) dt^2 + \frac{dr^2}{1 - \frac{2M}{r}} + r^2 \left(d\theta^2 + \sin^2\theta d\phi^2\right)$$

- The equations of motion for a photon

$$\ddot{x}^\mu + \Gamma^\mu_{\nu\sigma}\dot{x}^\nu \dot{x}^\sigma = 0$$

$$\dot{t} = \frac{E}{1 - \frac{2M}{r}}, \ \dot{\phi} = \frac{L}{r^2}, \ r^4\dot{\theta}^2 = \mathcal{K} - \frac{\cos^2\theta}{\sin^2\theta} L^2$$

$$\boxed{\frac{1}{E^2}\dot{r}^2 + b^2 V(r) = 1}$$

where, $b^2 = \frac{L^2}{E^2} + \frac{\mathcal{K}}{E^2} = \xi^2 + \eta$.

$$\boxed{V(r) = \frac{1}{r^2}\left(1 - \frac{2M}{r}\right)}$$

- b is the impact parameter.

- The effective potential has a maximum at $r = 3M$.
  $\Rightarrow$ Location of unstable circular orbit.
- $r = 3M$ is called a photon sphere.
- The critical impact parameter is $b_c = 3\sqrt{3}M$.

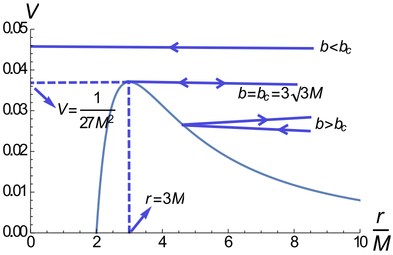

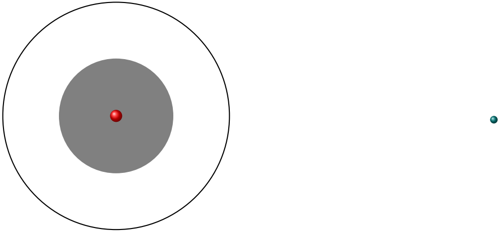

- The effective potential has a maximum at $r = 3M$.
  $\Rightarrow$ Location of unstable circular orbit.
- $r = 3M$ is called a photon sphere.
- The critical impact parameter is $b_c = 3\sqrt{3}M$.

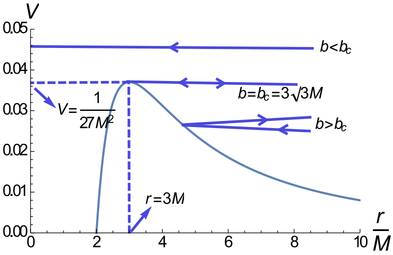

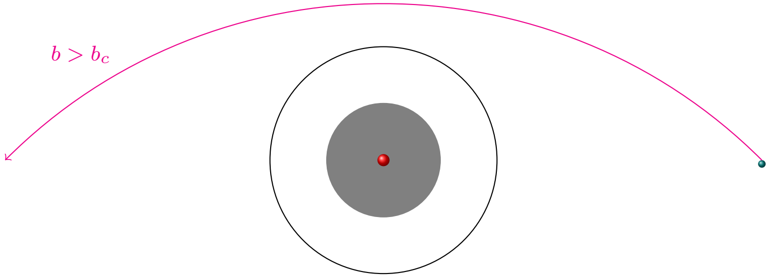

- The effective potential has a maximum at $r = 3M$.
  $\Rightarrow$ Location of unstable circular orbit.
- $r = 3M$ is called a photon sphere.
- The critical impact parameter is $b_c = 3\sqrt{3}M$.

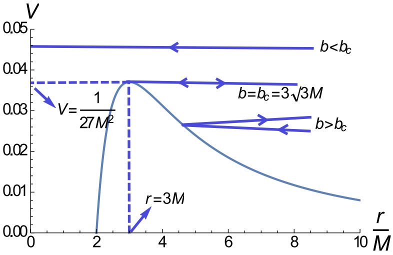

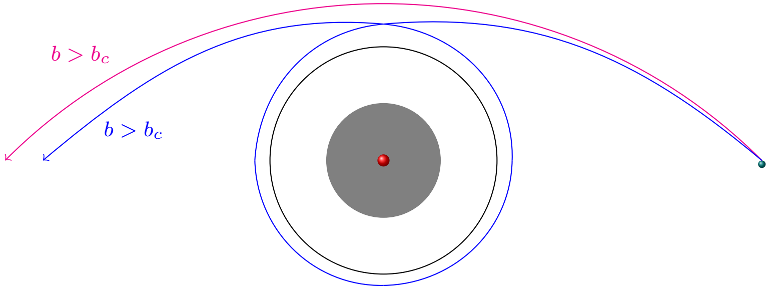

- The effective potential has a maximum at $r = 3M$.
  $\Rightarrow$ Location of unstable circular orbit.
- $r = 3M$ is called a photon sphere.
- The critical impact parameter is $b_c = 3\sqrt{3}M$.

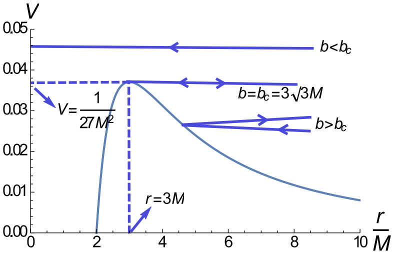

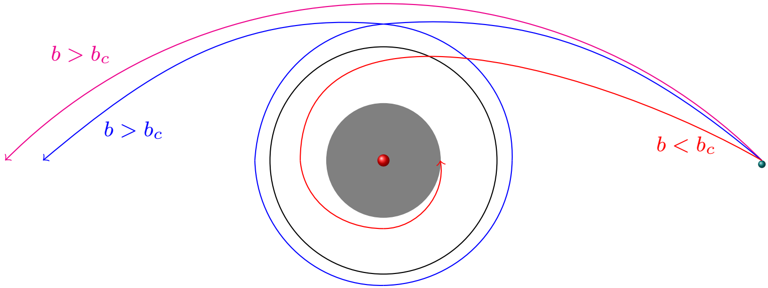

- The effective potential has a maximum at $r = 3M$.
  $\Rightarrow$ Location of unstable circular orbit.
- $r = 3M$ is called a photon sphere.
- The critical impact parameter is $b_c = 3\sqrt{3}M$.

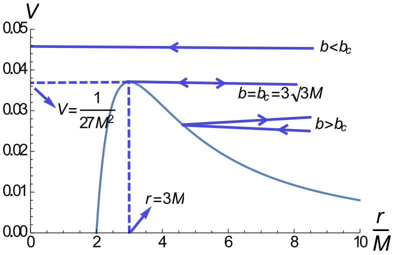

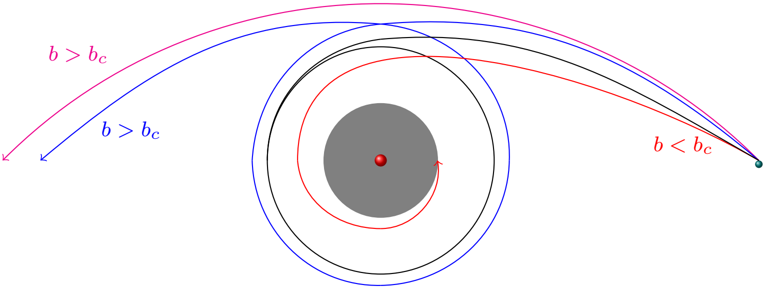

- The effective potential has a maximum at $r = 3M$.
  $\Rightarrow$ Location of unstable circular orbit.
- $r = 3M$ is called a photon sphere.
- The critical impact parameter is $b_c = 3\sqrt{3}M$.

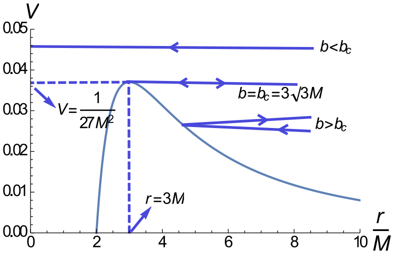

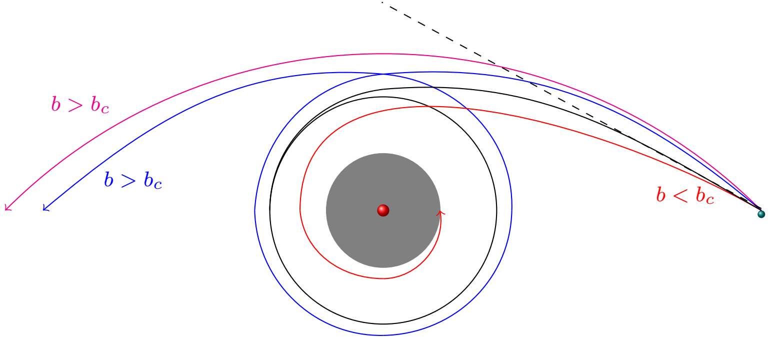

- The effective potential has a maximum at $r = 3M$.
  $\Rightarrow$ Location of unstable circular orbit.
- $r = 3M$ is called a photon sphere.
- The critical impact parameter is $b_c = 3\sqrt{3}M$.

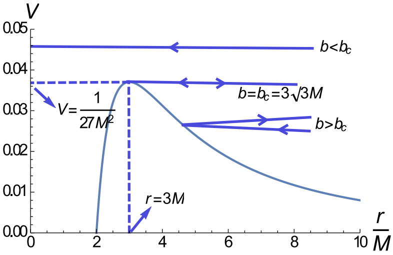

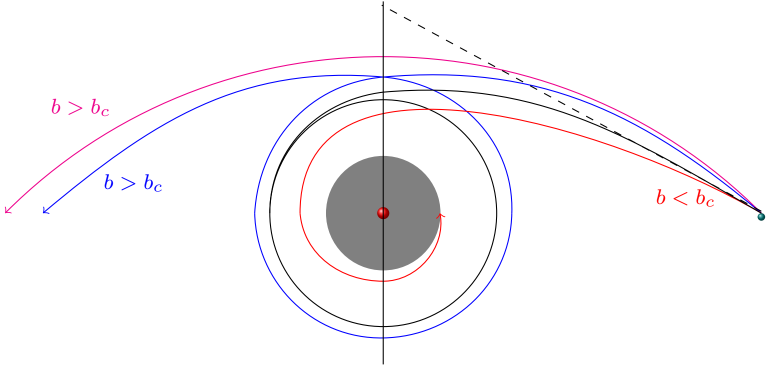

Naked singularity as an example

- The Joshi-Malafarina-Narayan (JMN) spacetimes describe the geometry around naked singularities.
- JMN-1 (P. S. Joshi, D. Malafarina, and R. Narayan, Class. Quantum Grav. **28**, 235018 (2011))

$$ds_1^2 = -(1 - M_0)\left(\frac{r}{R_b}\right)^{\frac{M_0}{1-M_0}} dt^2 + \frac{dr^2}{1 - M_0} + r^2\left(d\theta^2 + \sin^2\theta d\phi^2\right).$$

- It is matched to an exterior Schwarzschild geometry at $r = R_b$ where $2M = M_0 R_b$.

Naked singularity as an example

- The Joshi-Malafarina-Narayan (JMN) spacetimes describe the geometry around naked singularities.
- JMN-1 (P. S. Joshi, D. Malafarina, and R. Narayan, Class. Quantum Grav. **28**, 235018 (2011))

$$ds_1^2 = -(1-M_0)\left(\frac{r}{R_b}\right)^{\frac{M_0}{1-M_0}} dt^2 + \frac{dr^2}{1-M_0} + r^2\left(d\theta^2 + \sin^2\theta d\phi^2\right).$$

- It is matched to an exterior Schwarzschild geometry at $r = R_b$ where $2M = M_0 R_b$.

[**R. Shaikh**, P. Kocherlakota, R. Narayan, and P. S. Joshi, MNRAS **482**, 52-64 (2019)]

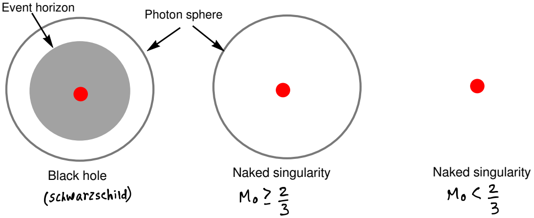

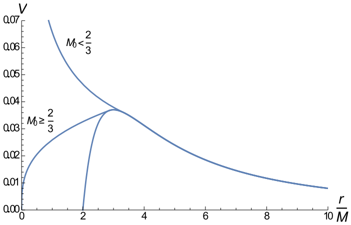

Figure: Schwarzschild and JMN-1

Naked singularity as an example

Shadows and images with spherical accretion

[**R. Shaikh**, P. Kocherlakota, R. Narayan, and P. S. Joshi, MNRAS **482**, 52-64 (2019)]

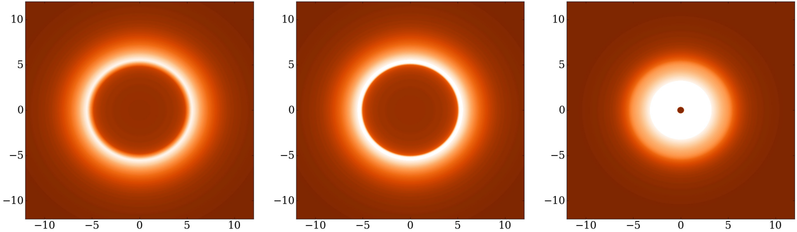

(a) Schwarzschild black hole (b) $M_0 = 0.7$, JMN-1 naked singularity (c) $M_0 = 0.6$, JMN-1 naked singularity

- Photon sphere exists for $M_0 \geq \frac{2}{3}$ $(R_b < 3M) \Rightarrow$ A shadow
- No photon sphere for $M_0 < \frac{2}{3}$ $(R_b > 3M) \Rightarrow$ No shadow

Our results in light of the EHT results of M87*

The Astrophysical Journal Letters, 875:L1 (17pp), 2019 April 10
https://doi.org/10.3847/2041-8213/ab0ec7

First M87 Event Horizon Telescope Results. I. The Shadow of the Supermassive Black Hole

The Event Horizon Telescope Collaboration
(See the end matter for the full list of authors.)
Received 2019 March 1; revised 2019 March 12; accepted 2019 March 12; published 2019 April 10

At the same time, it is more difficult to rule out alternatives to black holes in GR, because a shadow can be produced by any compact object with a spacetime characterized by unstable circular photon orbits (Mizuno et al. 2018). Indeed, while the Kerr metric remains a solution in some alternative theories of gravity (Barausse & Sotiriou 2008; Psaltis et al. 2008), non-Kerr black hole solutions do exist in a variety of such modified theories (Berti et al. 2015). Furthermore, exotic alternatives to black holes, such as naked singularities (Shaikh et al. 2019), boson stars (Kaup 1968; Liebling & Palenzuela 2012), and gravastars (Mazur & Mottola 2004; Chirenti & Rezzolla 2007), are admissible solutions within GR and provide concrete, albeit contrived, models. Some of such exotic compact objects can already be shown to be incompatible with our observations given our maximum mass prior. For example, the shadows of naked singularities associated with Kerr spacetimes with $|a_*| > 1$ are substantially smaller and very asymmetric compared to those of Kerr black holes (Bambi & Freese 2009). Also, some commonly used types of wormholes (Bambi 2013) predict much smaller shadows than we have measured.

The Astrophysical Journal Letters, 875:L5 (31pp), 2019 April 10
https://doi.org/10.3847/2041-8213/ab0f43

First M87 Event Horizon Telescope Results. V. Physical Origin of the Asymmetric Ring

The Event Horizon Telescope Collaboration
(See the end matter for the full list of authors.)
Received 2019 March 4; revised 2019 March 12; accepted 2019 March 12; published 2019 April 10

for M87. Similarly, for certain parameter ranges, the shadows of spherically symmetric naked singularities have been found to consist of a filled disk with no dark region[120] in the center (Shaikh et al. 2019); clearly, this class of models is ruled out. In

Our results in light of the EHT results of M87*

The Astrophysical Journal Letters, 875:L1 (17pp), 2019 April 10 https://doi.org/10.3847/2041-8213/ab0ec7

First M87 Event Horizon Telescope Results. I. The Shadow of the Supermassive Black Hole

The Event Horizon Telescope Collaboration
(See the end matter for the full list of authors.)
Received 2019 March 1; revised 2019 March 12; accepted 2019 March 12; published 2019 April 10

The Astrophysical Journal Letters, 875:L5 (31pp), 2019 April 10 https://doi.org/10.3847/2041-8213/ab0f43

First M87 Event Horizon Telescope Results. V. Physical Origin of the Asymmetric Ring

The Event Horizon Telescope Collaboration
(See the end matter for the full list of authors.)
Received 2019 March 4; revised 2019 March 12; accepted 2019 March 12; published 2019 April 10

for M87. Similarly, for certain parameter ranges, the shadows of spherically symmetric naked singularities have been found to consist of a filled disk with no dark region[120] in the center (Shaikh et al. 2019); clearly, this class of models is ruled out. In

At the same time, it is more difficult to rule out alternatives to black holes in GR, because a shadow can be produced by any compact object with a spacetime characterized by unstable circular photon orbits (Mizuno et al. 2018). Indeed, while the Kerr metric remains a solution in some alternative theories of gravity (Barausse & Sotiriou 2008; Psaltis et al. 2008), non-Kerr black hole solutions do exist in a variety of such modified theories (Berti et al. 2015). Furthermore, exotic alternatives to black holes, such as naked singularities (Shaikh et al. 2019), boson stars (Kaup 1968; Liebling & Palenzuela 2012), and gravastars (Mazur & Mottola 2004; Chirenti & Rezzolla 2007), are admissible solutions within GR and provide concrete, albeit contrived, models. Some of such exotic compact objects can already be shown to be incompatible with our observations given our maximum mass prior. For example, the shadows of naked singularities associated with Kerr spacetimes with $|a_*| > 1$ are substantially smaller and very asymmetric compared to those of Kerr black holes (Bambi & Freese 2009). Also, some commonly used types of wormholes (Bambi 2013) predict much smaller shadows than we have measured.

Horizonless compact objects can also cast black-hole-like shadows

A shadow does not always necessarily imply a black hole

Shadow observables

- The geometric center $(\alpha_c, 0)$:

$$\alpha_c = \frac{1}{A}\int \alpha dA$$

- The average radius R_{av}:

$$R_{av}^2 = \frac{1}{2\pi}\int_0^{2\pi} l^2(\phi)\, d\phi$$

- The deviation from circularity:

$$\Delta C = \frac{1}{R_{av}}\sqrt{\frac{1}{2\pi}\int_0^{2\pi} (l(\phi) - R_{av})^2\, d\phi}.$$

- The fractional deviation from Schwarzschild shadow

$$\delta = \frac{d_{sh}}{d_{sh,Sch}} - 1 = \frac{\Delta\theta_{sh}}{6\sqrt{3}\theta_g} - 1,$$

$$d_{sh} = 2R_{av}, \quad \Delta\theta_{sh} = \frac{d_{sh}}{D}, \quad \theta_g = \frac{M}{D}$$

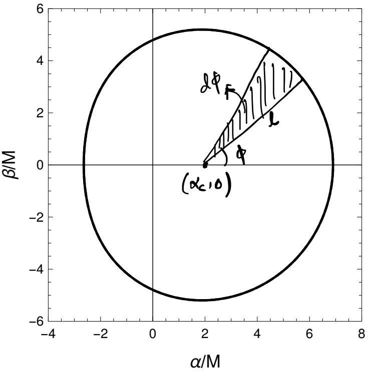

$$l(\phi) = \sqrt{(\alpha(\phi) - \alpha_c)^2 + \beta(\phi)^2}$$
$$\phi = tan^{-1}(\beta(\phi)/(\alpha(\phi) - \alpha_c))$$

Shadow observables

- The geometric center $(\alpha_c, 0)$:

$$\alpha_c = \frac{1}{A}\int \alpha dA$$

- The average radius R_{av}:

$$R_{av}^2 = \frac{1}{2\pi}\int_0^{2\pi} l^2(\phi)\, d\phi$$

- The deviation from circularity:

$$\Delta C = \frac{1}{R_{av}}\sqrt{\frac{1}{2\pi}\int_0^{2\pi}(l(\phi)-R_{av})^2\, d\phi}.$$

- The fractional deviation from Schwarzschild shadow

$$\delta = \frac{d_{sh}}{d_{sh,Sch}} - 1 = \frac{\Delta\theta_{sh}}{6\sqrt{3}\theta_g} - 1,$$

$$d_{sh} = 2R_{av}, \quad \Delta\theta_{sh} = \frac{d_{sh}}{D}, \quad \theta_g = \frac{M}{D}$$

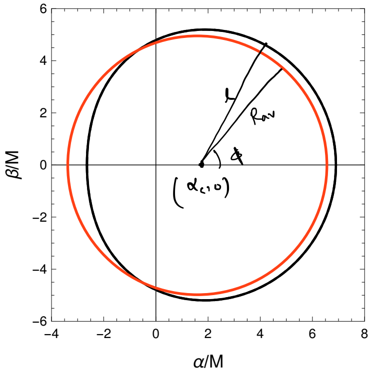

$$l(\phi) = \sqrt{(\alpha(\phi)-\alpha_c)^2 + \beta(\phi)^2}$$
$$\phi = tan^{-1}(\beta(\phi)/(\alpha(\phi)-\alpha_c))$$

M87*

- $D = (16.8 \pm 0.8)$, $M = (6.5 \pm 0.7) \times 10^9 M_\odot$, $\theta_o = 17^\circ$
- The observed values: $\Delta\theta_{sh} = 42 \pm 3$ μas and $\Delta C < 0.1$ (deviation from circularity is less than 10%) [a]
- The dimensionless diameter should be

$$\frac{d_{sh}}{M} = \frac{D\Delta\theta_{sh}}{M} = 11.0 \pm 1.5.$$

- The EHT collaboration found the spin to be $0.5 \leq a/M \leq 0.94$.

[a] The Event Horizon Telescope Collaboration, Astrophys. J. Lett. 875, L1 (2019).

M87*

- $D = (16.8 \pm 0.8)$, $M = (6.5 \pm 0.7) \times 10^9 M_\odot$, $\theta_o = 17^\circ$
- The observed values: $\Delta\theta_{sh} = 42 \pm 3\ \mu$as and $\Delta C < 0.1$ (deviation from circularity is less than 10%) [a]
- The dimensionless diameter should be

$$\frac{d_{sh}}{M} = \frac{D\Delta\theta_{sh}}{M} = 11.0 \pm 1.5.$$

- The EHT collaboration found the spin to be $0.5 \leq a/M \leq 0.94$.

[a] The Event Horizon Telescope Collaboration, Astrophys. J. Lett. 875, L1 (2019).

Sgr A*

- The observed value: $\Delta\theta_{sh} = 48.7 \pm 7.0\ \mu$as and $\theta_0 > 50^\circ$ is disfavoured. [a]
- The measured value of the fractional deviation (from Schwarzschild shadow)

$$\delta = \begin{cases} -0.08^{+0.09}_{-0.09} & \text{(VLTI)} \\ -0.04^{+0.09}_{-0.10} & \text{(Keck)} \end{cases}.$$

- At the 1σ credible level, $-0.17 \leq \delta \leq 0.01$ (VLTI) and $-0.14 \leq \delta \leq 0.05$ (Keck).
- For Kerr black hole $-0.08 \leq \delta \leq 0$, considering all spins and inclination angles.

[a] The Event Horizon Telescope Collaboration, Astrophys. J. Lett. 930, L12 (2022).

Constraint on rotating regularized Schwarzschild spacetime

Constraints from M87* results

[**R. Shaikh**, K. Pal, K. Pal, and T. Sarkar, MNRAS **506**, 1229-1236 (2021)]

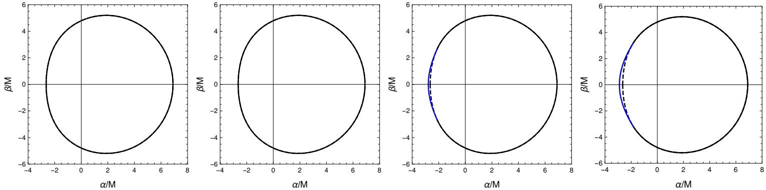

(d) $r_0 < r_+$ (e) $r_0/r_+ = 1.05$ (f) $r_0/r_+ = 1.25$ (g) $r_0/r_+ = 1.35$

- The non-singular black hole case is always consistent with the observations.

- Observed values:
  $d_{sh}/M = 11.0 \pm 1.5$ and
  $\Delta C < 0.1$
- The maximum value of r_0 must lies within the range
  $2.54 \leq r_{0,max}/r_+ \leq 3.51$

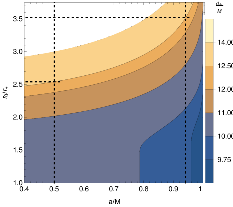

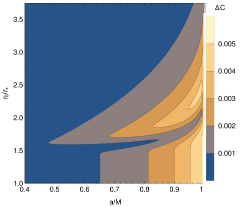

Constraint on rotating regularized Schwarzschild spacetime

Constraint from Sgr A* result

[**R. Shaikh**, MNRAS **523**, 375-384 (2023)]

- The observed value: $\delta \Rightarrow -0.17 \leq \delta \leq 0.01$ (VLTI) and $-0.14 \leq \delta \leq 0.05$ (Keck)
- For Kerr, $-0.08 \leq \delta \leq 0$
- For a given a and θ_o, the shadow diameter is the same as Kerr when $r_0 \leq r_{0c}$.

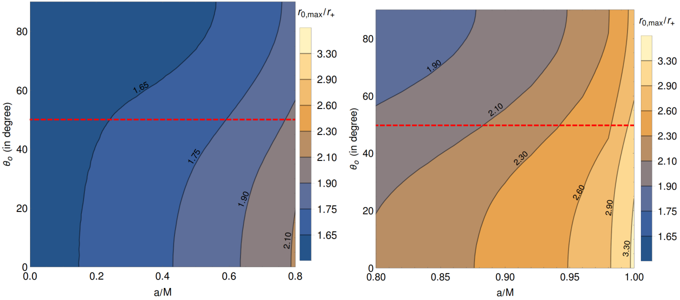

(j) VLTI

(k) VLTI

- VLTI bound $\Rightarrow$ For $0 \leq a/M \leq 1$, $1.636 \lesssim r_{0,max}/r_+ \lesssim 3.059$ when $\theta = 46^\circ$.

Constraint on rotating regularized Schwarzschild spacetime

Constraint from Sgr A* result

[**R. Shaikh**, MNRAS **523**, 375-384 (2023)]

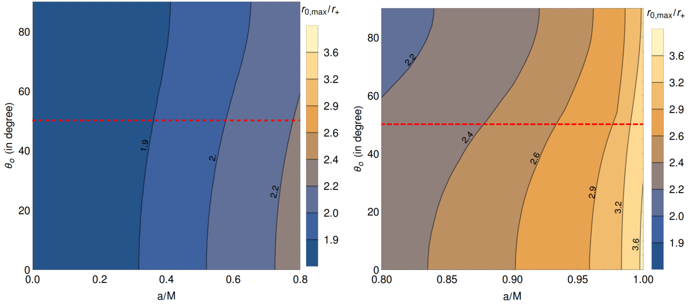

(l) Keck (m) Keck

- Keck bound $\Rightarrow$ For $0 \leq a/M \leq 1$, $1.848 \lesssim r_{0,max}/r_+ \lesssim 3.492$ when $\theta_o = 46^\circ$.

Constraint on rotating regularized Schwarzschild spacetime

Combined constraint from M87* and Sgr A* results

$2.54 \leq r_{0,max}/r_+ \leq 3.51$	(M87*)	$4.71M \leq r_{0,max} \leq 4.74M$
$1.636 \lesssim r_{0,max}/r_+ \lesssim 3.059$	(Sgr A*, VLTI)	$3.06M \leq r_{0,max} \leq 3.27M$
$1.848 \leq r_{0,max}/r_+ \leq 3.492$	(Sgr A*, Keck)	$3.49M \leq r_{0,max} \leq 3.70M$

- $r_0 \leq r_{0,max}$ is allowed.
- The metric is consistent with the observed shadows of both M87* and Sgr A* if $r_0 \leq 3.09M$, irrespective of the allowed spin value.

Constraints on rotating regularized JNW spacetime

Constraints from M87* results

[K. Pal, K. Pal, **R. Shaikh**, and T. Sarkar, JCAP 11 (2023) 060]

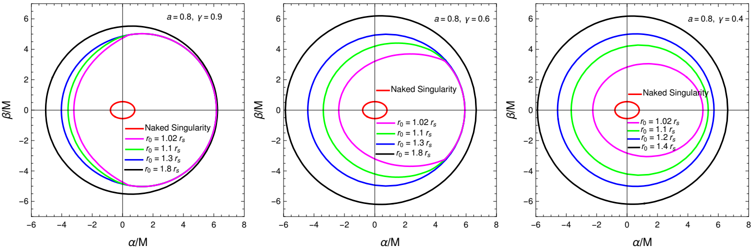

- For the naked singularity case ($r_0 \leq r_s$)

$$\frac{\alpha^2}{a^2} + \frac{\beta^2}{a^2 \cos^2 \theta_o} = 1$$

$\Rightarrow d_{sh}/M = 2\sqrt{\cos \theta_o}\,(a/M)$

$\Rightarrow$ Much smaller than the observed value.

- The naked singularity case is not consistent with the observations.

Constraints on rotating regularized JNW spacetime

Constraints from M87* results

[K. Pal, K. Pal, **R. Shaikh**, and T. Sarkar, JCAP 11 (2023) 060]

- The wormhole case ($r_0 > r_s$)

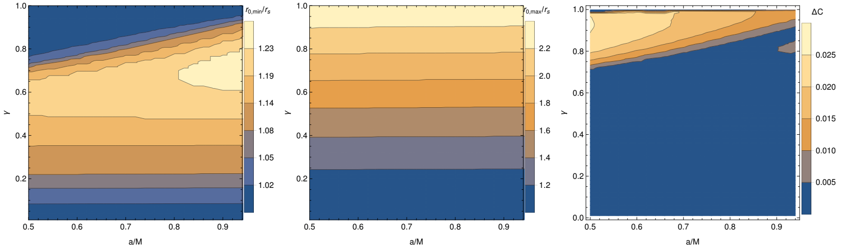

- For a given γ and a/M, the allowed range is $r_{0,min} \leq r_0 \leq r_{0,max}$.

Constraints on rotating regularized JNW spacetime

Constraints from Sgr A* results

[K. Pal, K. Pal, **R. Shaikh**, and T. Sarkar, JCAP 11 (2023) 060]

VLTI $\Rightarrow$

Keck $\Rightarrow$

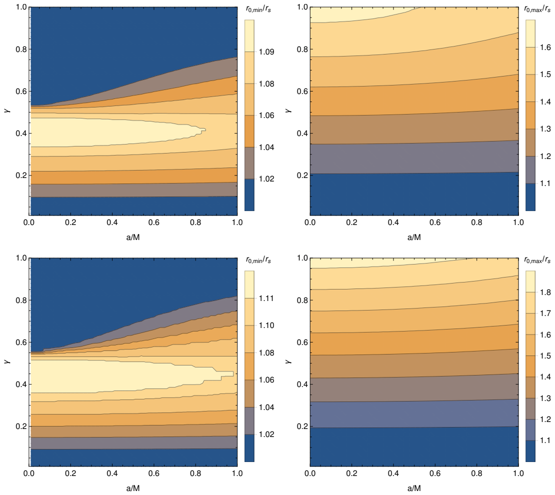

- For a given γ and a/M, the allowed range is $r_{0,min} \leq r_0 \leq r_{0,max}$.

Broad conclusions

- Some compact objects which do not have event horizons can also cast shadows similar to black holes, thereby acting as black hole mimickers.

  $\Rightarrow$ A Shadow does not always necessarily imply a black hole.

- The EHT results can be used to constrain parameters of these black hole mimickers.

- We have considered two black hole mimickers, namely the rotating regularized Schwarzschild and JNW spacetimes, and constrained them.
  - The non-singular black hole case is always consistent with the observed shadow.
  - The naked singularity case is always inconsistent.
  - The wormhole case is consistent with the observed shadow for some parameter ranges.

Broad conclusions

- Some compact objects which do not have event horizons can also cast shadows similar to black holes, thereby acting as black hole mimickers.

  $\Rightarrow$ A Shadow does not always necessarily imply a black hole.

- The EHT results can be used to constrain parameters of these black hole mimickers.
- We have considered two black hole mimickers, namely the rotating regularized Schwarzschild and JNW spacetimes, and constrained them.
  - The non-singular black hole case is always consistent with the observed shadow.
  - The naked singularity case is always inconsistent.
  - The wormhole case is consistent with the observed shadow for some parameter ranges.

Thank You